

## Supporting Information

# The Onset of Aerosol Au Nanoparticle Crystallization: Accretion & Explosive Nucleation

*Yi Wang<sup>1,2</sup>, Eirini Goudeli<sup>3\*</sup>*

<sup>1</sup>Particle Technology Laboratory, Department of Mechanical and Process Engineering, ETH  
Zürich, Zürich, CH-8092, Switzerland

<sup>2</sup>Center for Combustion Energy, Key Laboratory of Thermal Science and Power Engineering  
of Ministry of Education, Department of Energy and Power Engineering, Tsinghua  
University, Beijing 100084, China

<sup>3</sup>Department of Chemical Engineering, University of Melbourne, Melbourne, 3010, Australia

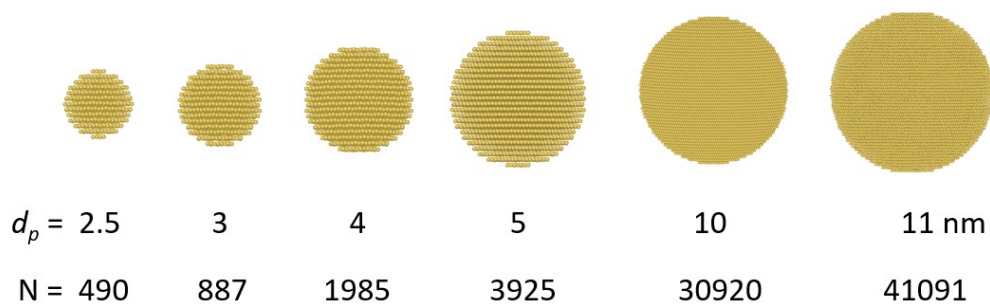


**Figure S1.** Snapshots of initial Au nanoparticles with corresponding diameter ( $d_p$ ) and number of Au atoms (N).

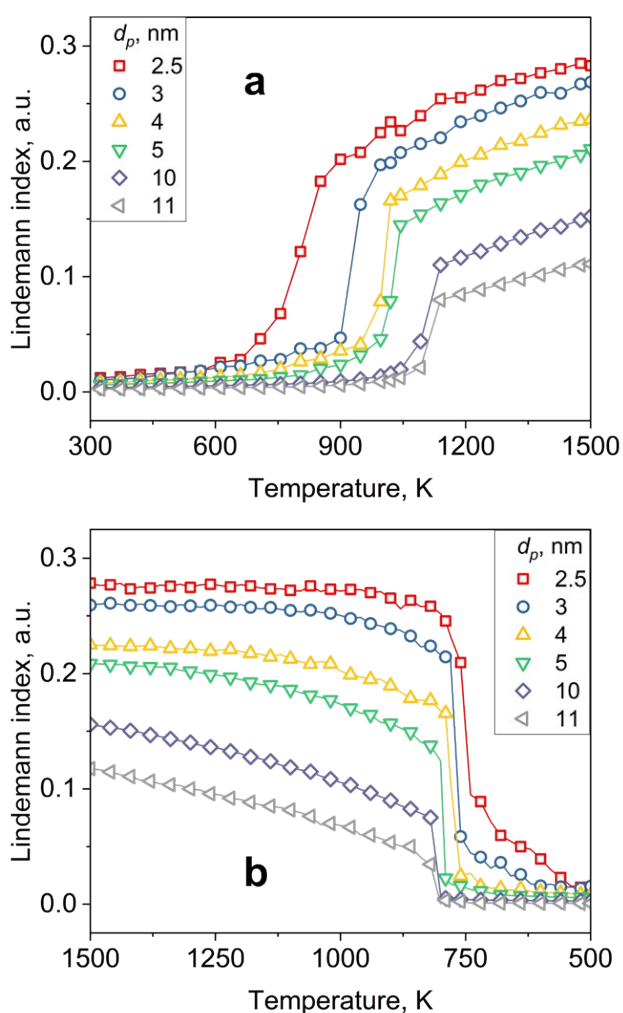


**Figure S2.** Evolution of the average Lindemann index of Au particles of various diameters as a function of temperature during heating from 300 to 1500 K at a heating/cooling rate of 100 K/ns.

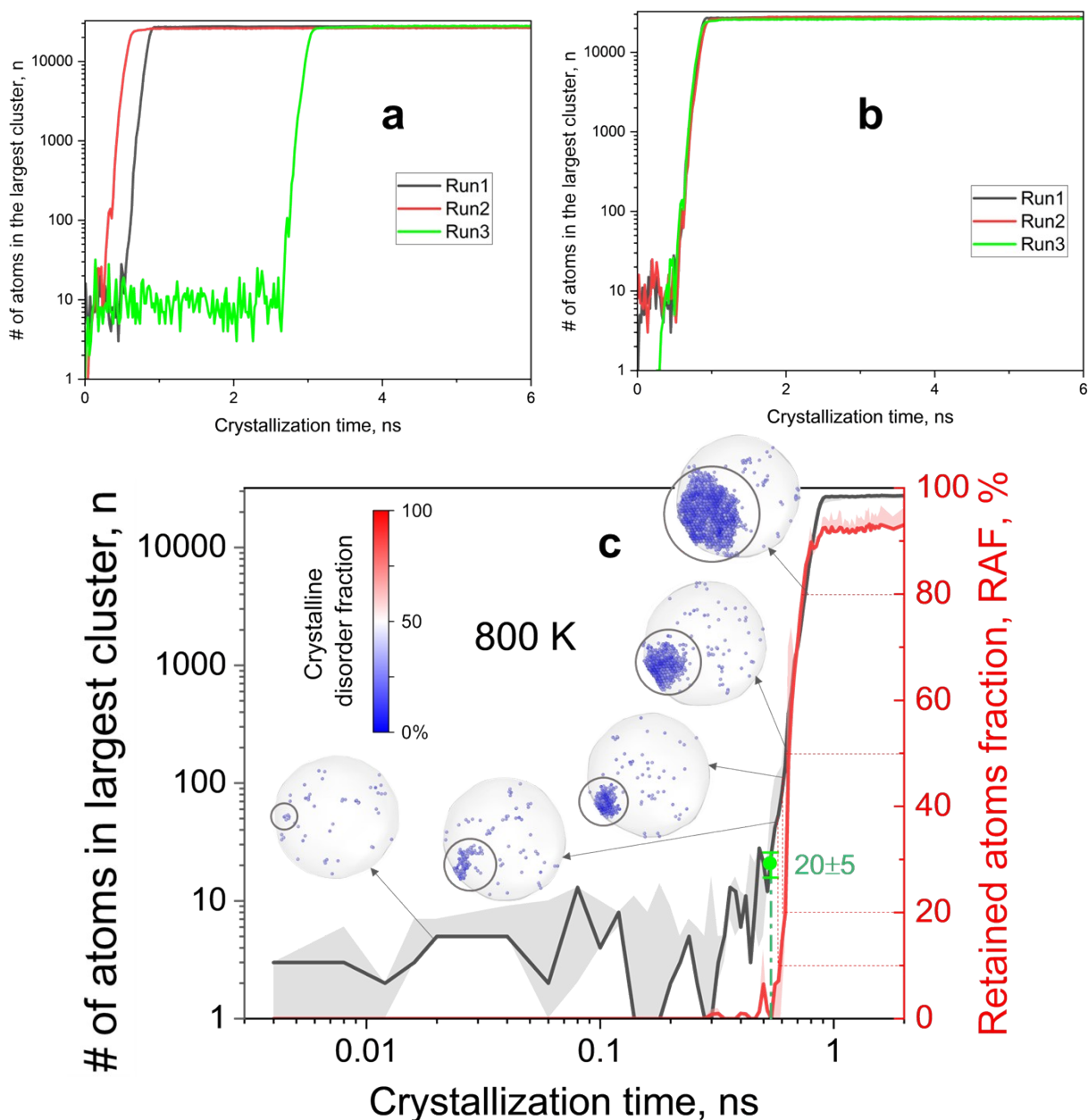


**Figure S3.** The evolution of the largest cluster size,  $n$ , during crystallization at 800 K of a 10 nm Au nanoparticle with three different MD simulations before (a) and after (b) been overlaid to match their crystallization onset. Average  $n$  and RAF are shown in (c) with shades representing variations among three runs, with the 3D snapshots of only the crystalline atoms at RAF = 10, 20, 50, 80%.

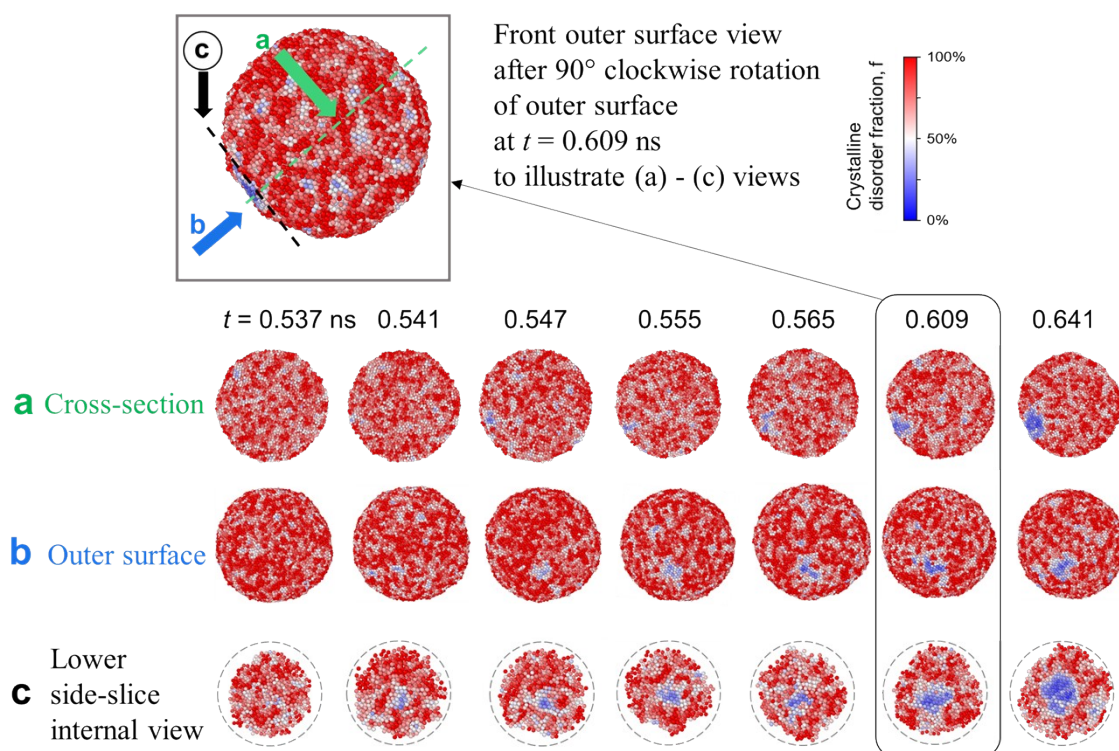


**Figure S4.** Snapshots of a 10 nm Au nanoparticle undergoing isothermal crystallization at 800 K during  $t = 0.537$  to 0.641 ns illustrating the onset of crystallization in (a) cross-section view crossing through the critical nucleus of Figure 2a insets, (b) outer surface view and (c) side-slice view of the lower part from the internal, colored by their local crystalline disorder fractions after normalization.

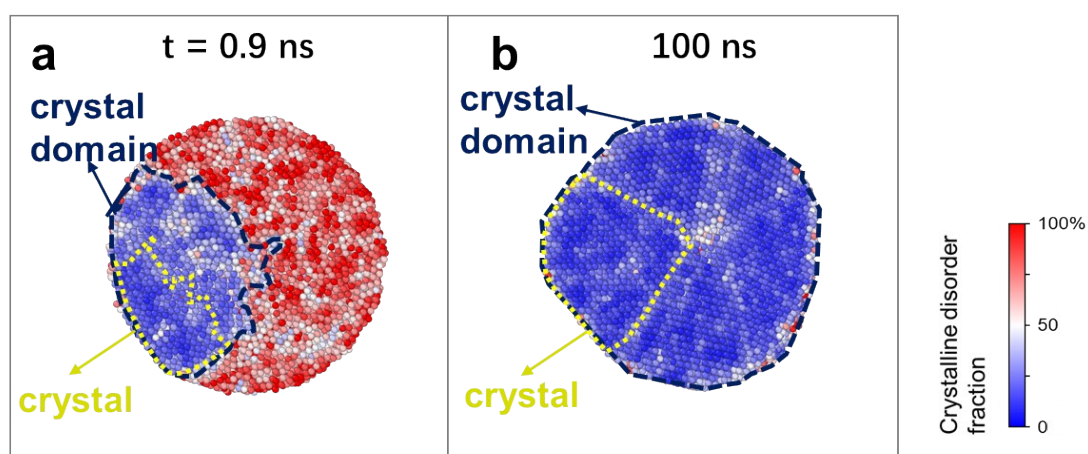


**Figure S5.** A demonstration of the distinction between “crystal” and “crystal domain” using two snapshots of cross-sections of 10 nm Au particle crystallizing at 800 K at 0.9 and 100 ns. When there are several crystals with clear boundaries, they are referred to as crystal domains.

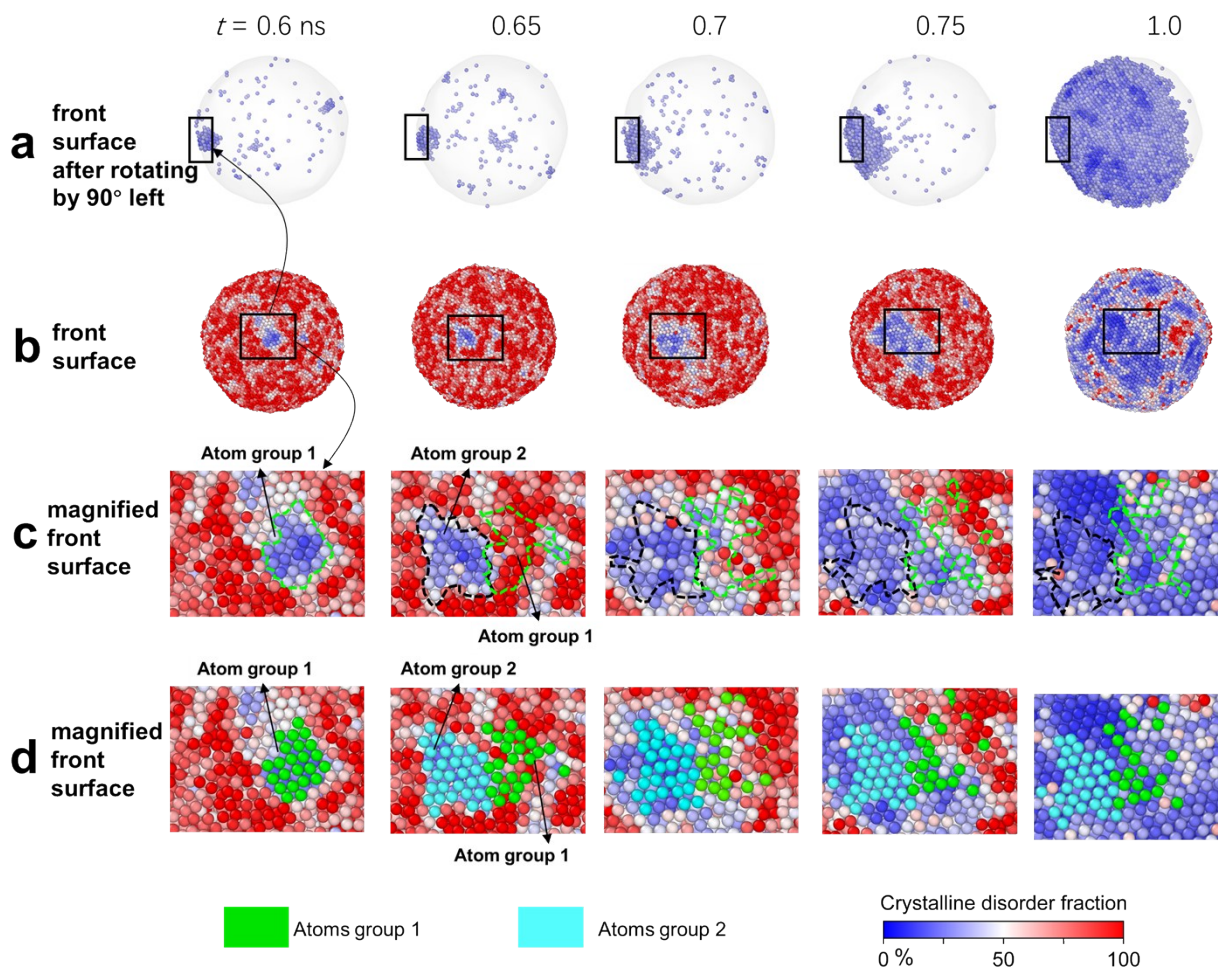


**Figure S6.** Snapshots from different views of initially amorphous Au nanoparticle undergoing isothermal crystallization at 800 K with  $d_p = 10$  nm at  $t = 0.6 - 1.0$  ns illustrating the dynamics of the atoms constituting a nucleus at the surface. (a) front surface view of 3D projection of crystals in the particle after rotating by  $90^\circ$  to the left, (b) front surface view of the whole nanoparticle (c) magnified local front surface view with atoms of two groups marked by dash circles, (d) magnified local front surface view with atoms of two groups highlighted by green and blue.

The dynamic formation and dissolution of atoms in crystalline state can still take place once the critical cluster size has been reached. At  $t = 0.6$  ns, the first group of atoms at crystalline state appears at the surface (Figure 2). These atoms are marked green (Figure S5c, d: atom group 1). Shortly after at 0.65 ns, new crystal forms in the nearby region which are marked blue (Figure

S5c, d:  $t = 0.65$  ns, atom group 2) while the atoms composing the first group become amorphous (atom group 1 are red in Figure S5c, d). The crystal grows larger at  $t = 0.7$  ns, with the atoms from group 2 still in crystalline state and some of atoms from group 1 transform to crystalline again (the corresponding light blue atoms in Figure S5c, d). Subsequently, the amorphous atoms within atom group 1 undergo gradual transformation back into crystalline (Figure S5c, d:  $t = 0.7 - 1$  ns) as a result of the expanding crystal domain (Figure S5a, b:  $t = 0.7 - 1$  ns). Over time, the fraction of unstable crystalline atoms steadily diminishes, which is evidenced by the increasing RAF (Figure 2b).

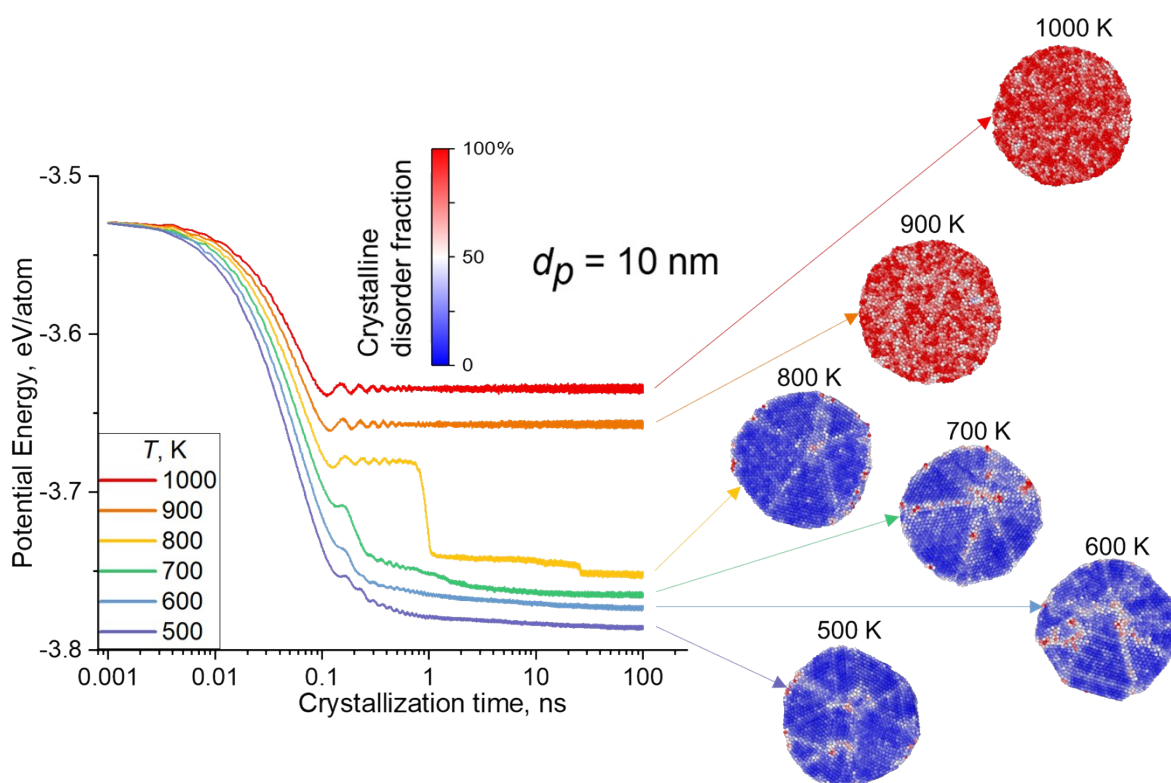


**Figure S7.** Evolution of potential energy per Au atom of initially amorphous Au nanoparticles ( $d_p = 10$  nm, obtained by heating to 1500 K) undergoing isothermal crystallization at  $T = 500, 600, 700, 800, 900, 1000$  K and their corresponding snapshots of cross-sections after 100 ns, colored by local crystalline disorder.

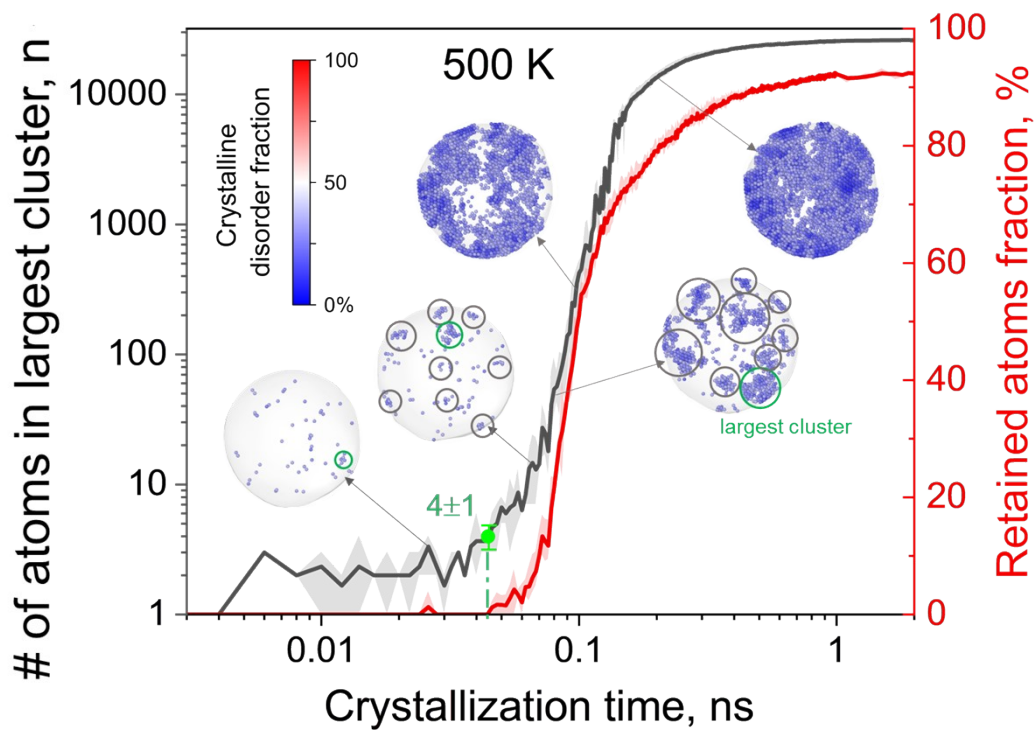


**Figure S8.** The evolution of the largest cluster size and RAF during crystallization at 500 K of a 10 nm Au nanoparticle after averaging three parallel MD simulation runs with 3D snapshots of only the crystalline atoms.

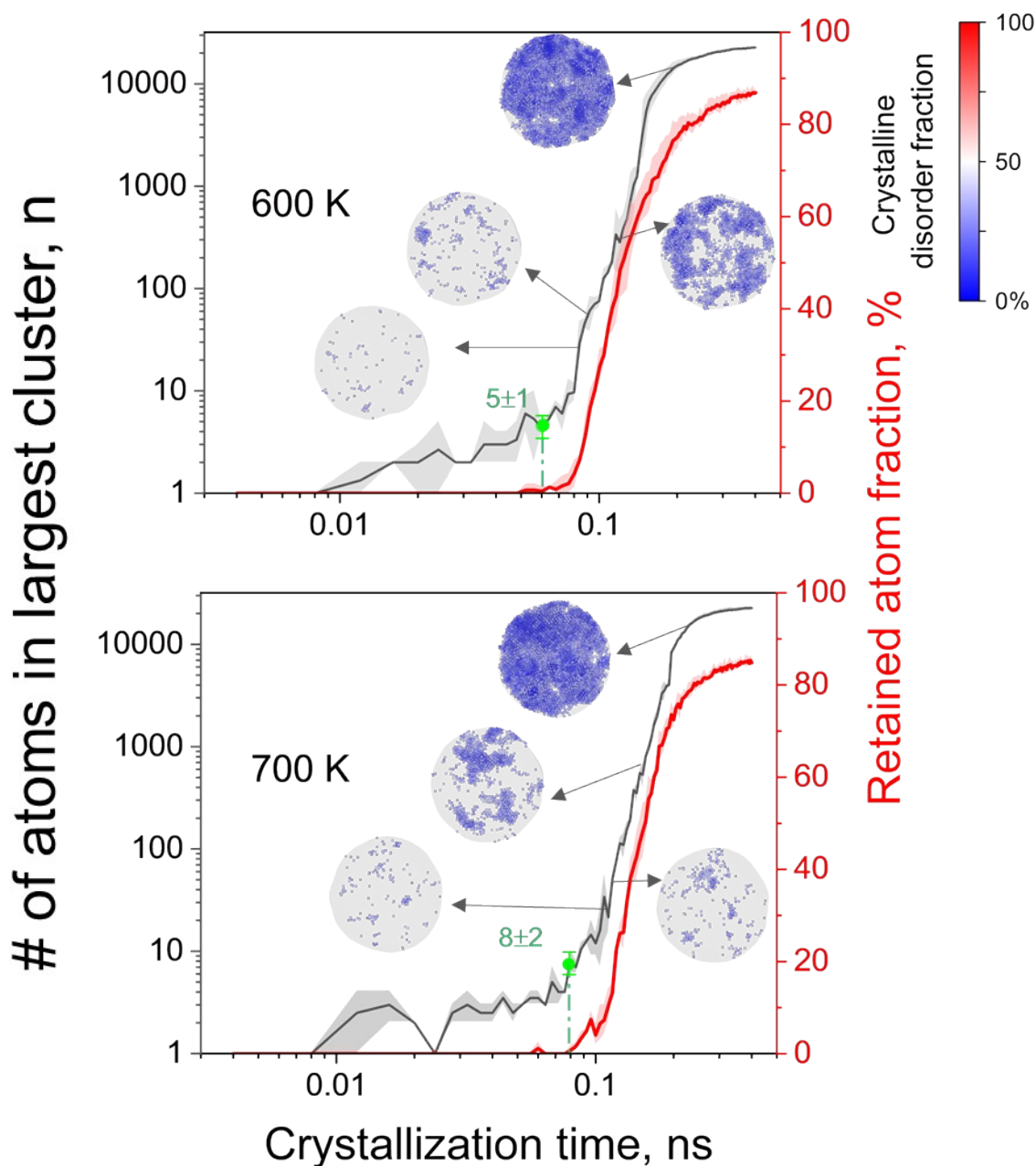


**Figure S9.** Number of atoms in the largest cluster (black lines, left axis) and its retained atoms fraction (RAF, blue lines, right axis) of a 10 nm Au particle at (a) 600 and (b) 700 K after averaging three parallel MD simulation runs with 3D snapshots of only the crystalline atoms at RAF = 10, 20, 50, 80%.



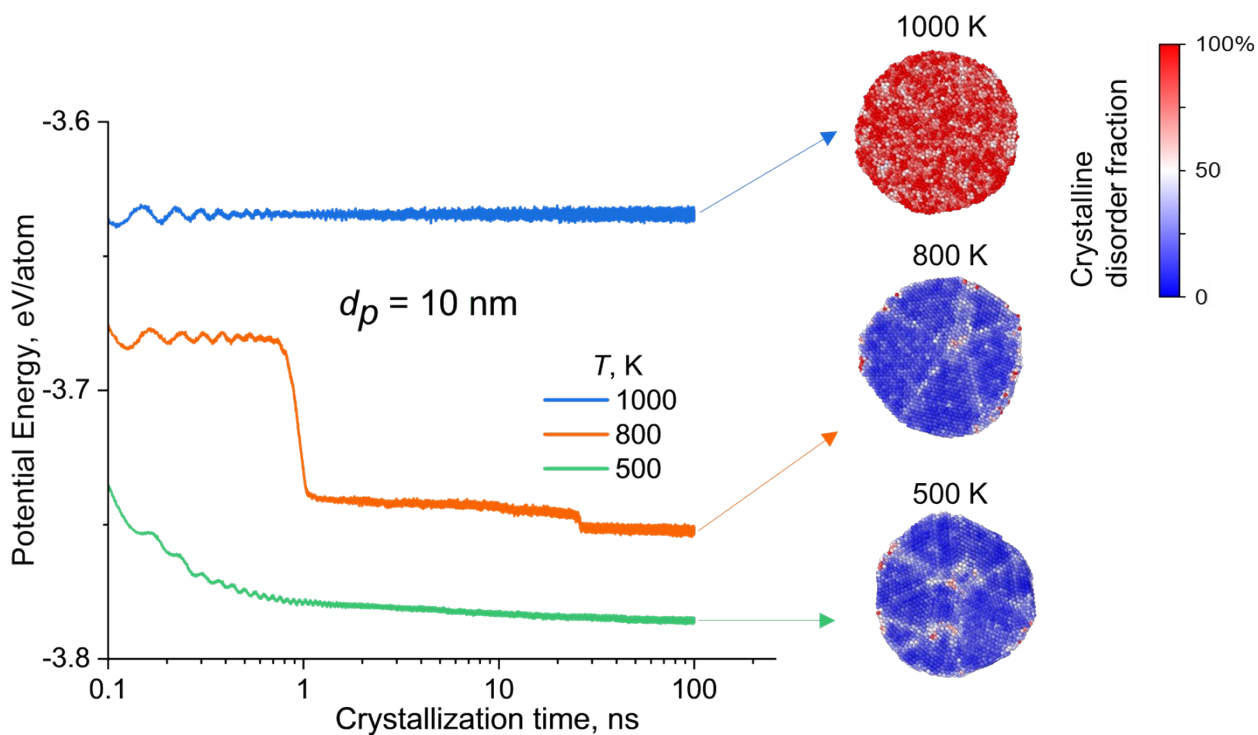


**Figure S10.** Evolution of potential energy per Au atom of initially amorphous Au nanoparticles ( $d_p = 10$  nm) undergoing isothermal crystallization at  $T = 500$ , 800, and 1000 K, and their corresponding final cross-sections. They are colored by the local crystalline disorder fraction after normalization, with red indicating completely amorphous and blue indicating perfect FCC or HCP crystals.

At 1000 K, the potential energy remains at a plateau until the end of the 100 ns simulation. As this temperature is closer to the melting point of the 10 nm particle, the atoms have high mobility and the nanoparticle exhibits high free energy difference from the crystalline state, making it harder to surmount the crystallization energy barrier and form supercritical nuclei. Thus, the chance for crystallization is very small within this timeframe and temperature. Therefore, there is no phase transition and the particle remains amorphous as shown by its nearly all-red final cross-section. This is consistent with simulations of smaller nanoparticles<sup>27</sup> (i.e. consisting of 1157 Au atoms, around 3.3 nm in diameter) at  $T > 740$  K, which had a lower

$T_f$ , and failed to crystallize within 1 ns. At  $T = 800$  K, as already shown in Figure 2a, the potential energy exhibits two distinct drops that are connected with nucleation ( $t = 1$  ns) and crystal domain formation (26 ns). The close proximity between the crystallization temperature of 800 K and the  $T_f$  (805 K for  $d_p = 10$  nm, Figure 1) increases the chance for the particle to solidify as detailed in Figure 2 and above discussion. In contrast, at  $T = 500$  K, deep into the solid phase region, crystallization is more favored thermodynamically. Thus, the potential energy drops much faster and lower than at 1000 and 800 K, resulting in full crystallization of the particle with several small and large crystals indicated by the multiple dark blue regions separated by the white shaded crystal boundaries, a characteristic of explosive nucleation.

At 800 K, there is a time-lag before crystallization shown by the delay of potential energy drop for  $d_p = 5 - 10$  nm (Figures S9, S10) compared with  $T = 500$  K. Their atoms have enough time to diffuse to positions of lower potential energy and more ordered orientations before crystalline transition happens, thus producing larger crystals. This can also be proved by the smallest crystal number (Figure S16a, yellow line) and largest crystal size (Figure S16b, yellow line) at  $T = 800$  K compared with other temperatures.

The time for crystallization increases with increasing temperature as shown by the time needed for the potential energy to reach a plateau, consistent with crystallization of Cu-Au alloys (Quoc et al., 2022), where increasing temperature inhibits crystallization. The further below  $T_f$ , the faster the nanoparticles crystallize. It is most impressive that once crystallization takes place at 50 K below the  $T_f$ , the number and size of crystals is nearly the same. For example, about 15 crystals of 2.5 nm each in a 5 nm Au particle were formed for crystallization of any temperature from 500 to 750 K (Figure S16b).

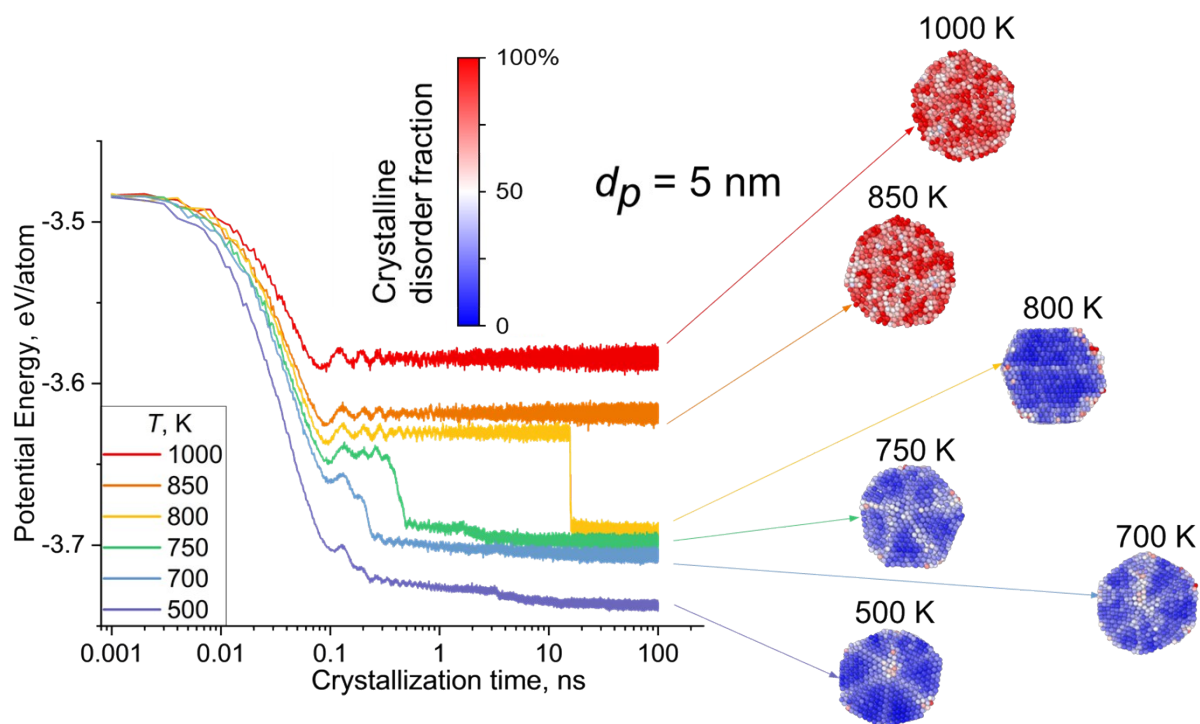


**Figure S11.** Evolution of potential energy per Au atom of initially amorphous Au nanoparticles ( $d_p = 5$  nm) undergoing isothermal crystallization at  $T = 500, 700, 750, 800, 850, 1000$  K and their corresponding snapshots of cross-sections after 100 ns, colored by local crystalline disorder.

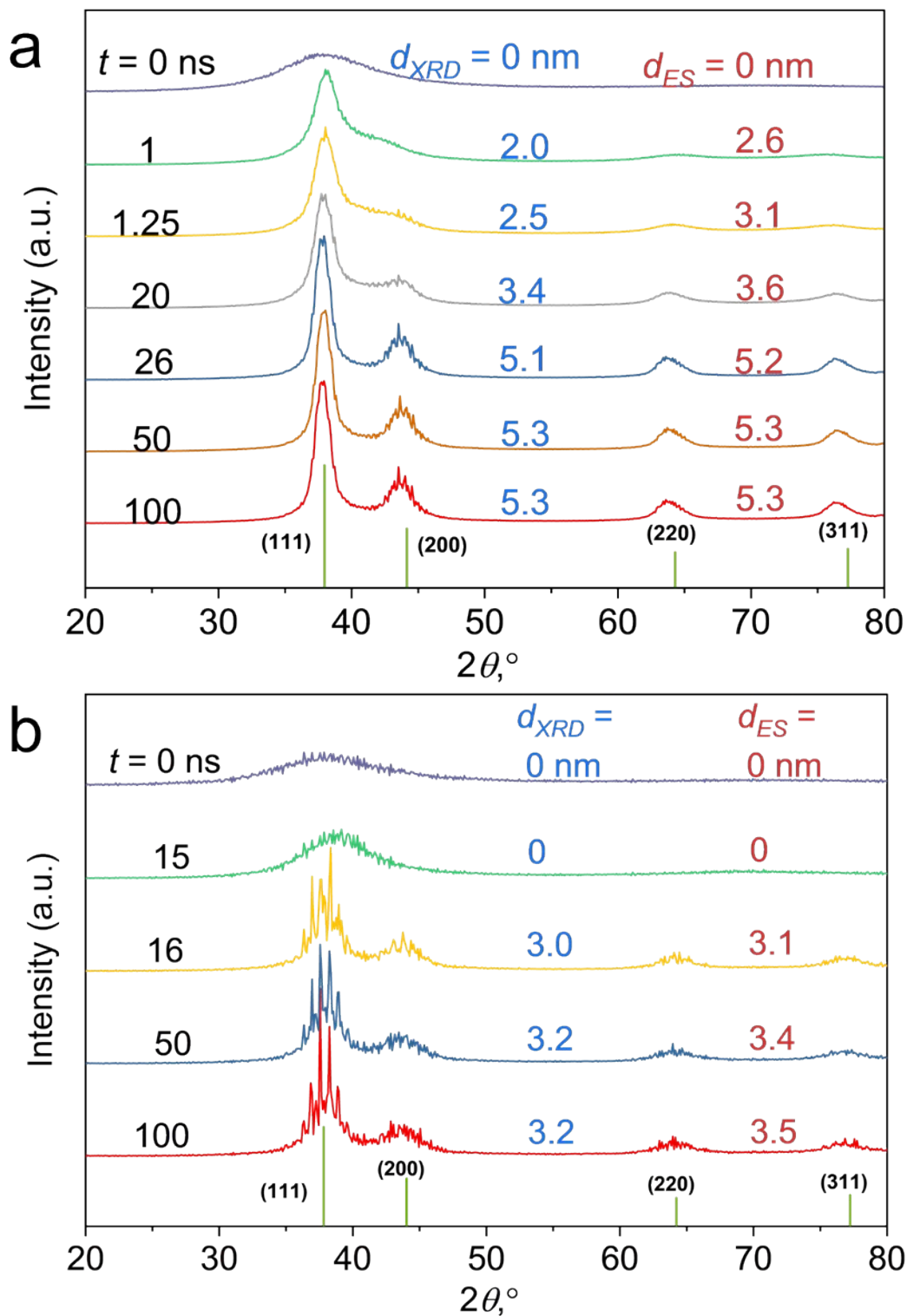


**Figure S12.** Evolution of XRD patterns of a) 10 and b) 5 nm Au nanoparticles undergoing crystallization at  $T = 800$  K with the corresponding time steps  $t$  and crystal size,  $d_{XRD}$  calculated by analyzing the XRD patterns and  $d_{ES}$  by direct tracing of trajectories. Main crystal planes of perfect Au crystal from database are labeled.

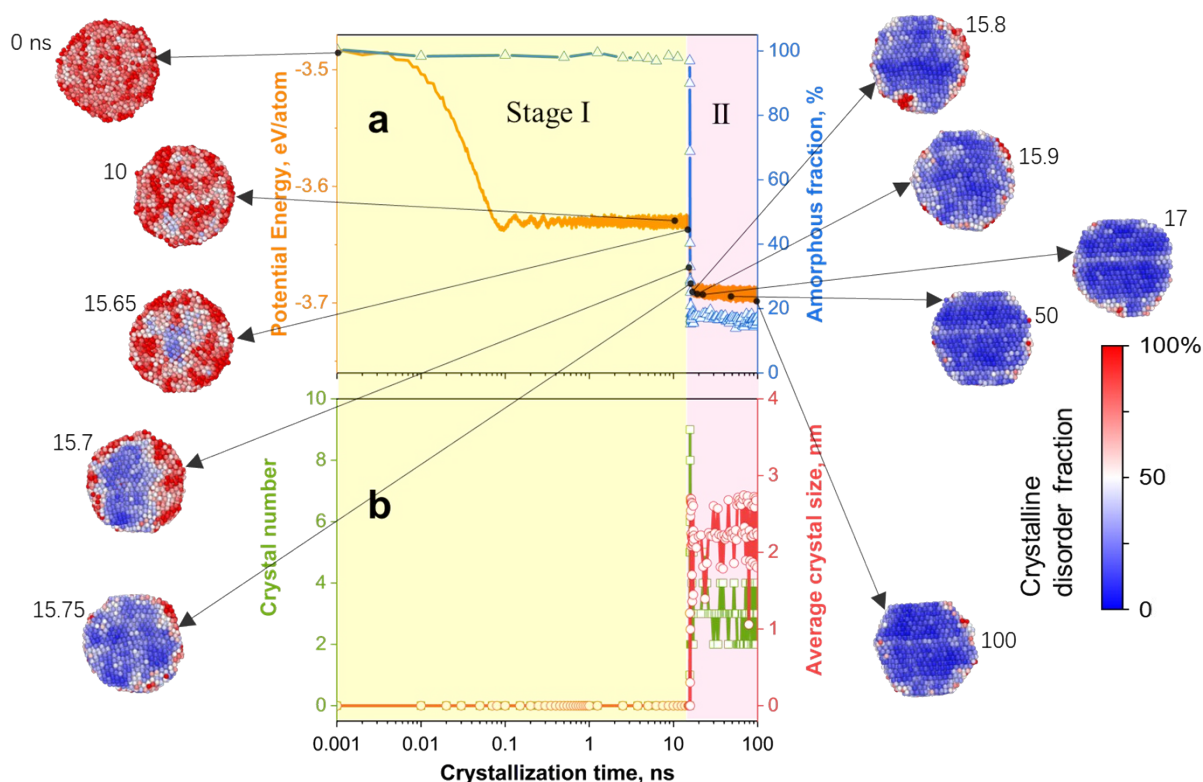


**Figure S13.** Cross-section snapshots during crystallization at 800 K for 100 ns, colored by the local crystalline disorder after normalization. Evolution of (a) average potential energy per Au atom (brown line) and amorphous fraction of a 5 nm Au nanoparticle (blue triangles) as well as its (b) number of crystals (green squares) and average crystal size (red circles) along with crystallization proceeds in two stages: (I) subcritical Au cluster formation; (II) supercritical Au crystal formation and growth by accretion.

The drop of the amorphous fraction lags behind that of the potential energy, as the amorphous fraction depends on local orientation symmetries (Eslami et al., 2018), which can only be influenced once the process of atomic rearrangement is completed. Despite the difference in size, both the 5 nm and 10 nm Au particle underwent a transformation from an initially 100% amorphous state to that of approximately 10%. The evolution of potential energy and amorphous fraction is similar to that reported in the literature for seeded isothermal

crystallization of Au nanoparticles,<sup>25</sup> which resulted in a final crystalline fraction of 80% (or amorphous fraction is below 20%) within 1 ns.

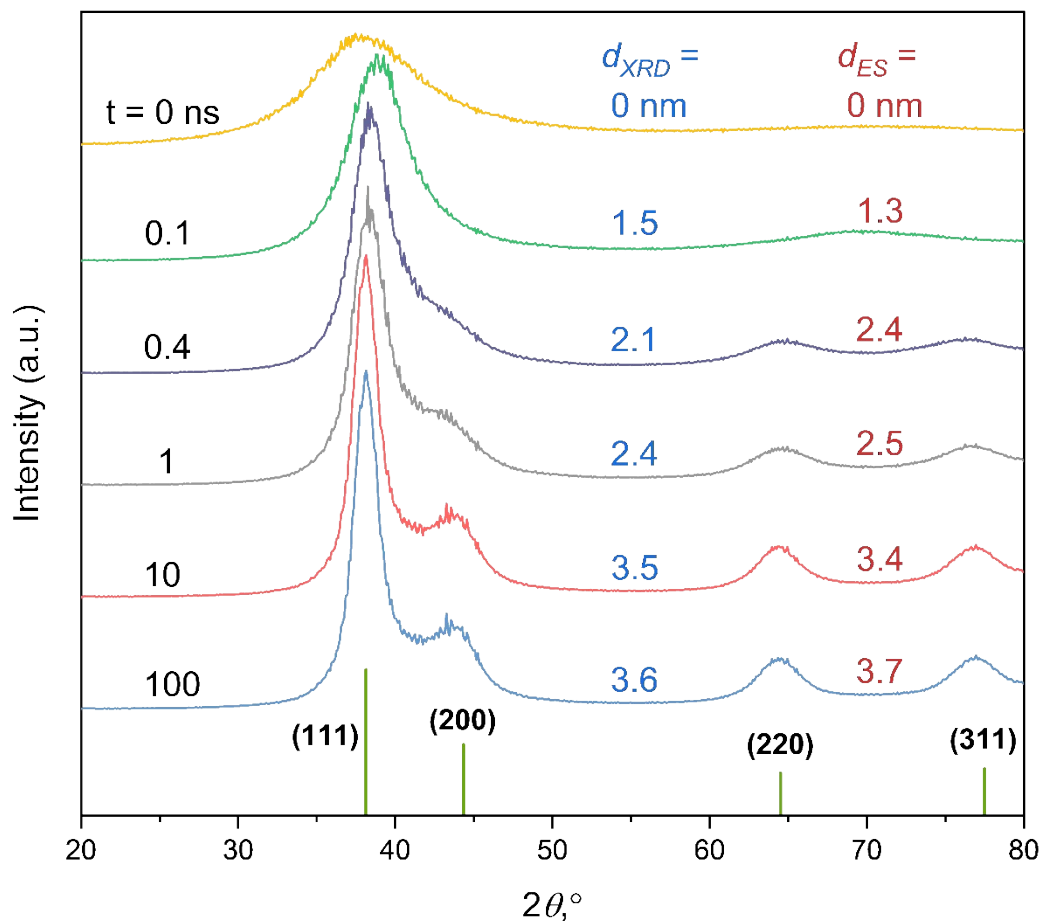


**Figure S14.** Evolution of XRD patterns of 10 nm Au nanoparticles undergoing isothermal crystallization at  $T = 500$  K with the corresponding time steps  $t$  and crystal size,  $d_{XRD}$  calculated by analyzing the XRD patterns and  $d_{ES}$  by direct tracing of trajectories. Main crystal planes of perfect Au crystal from database are labeled.

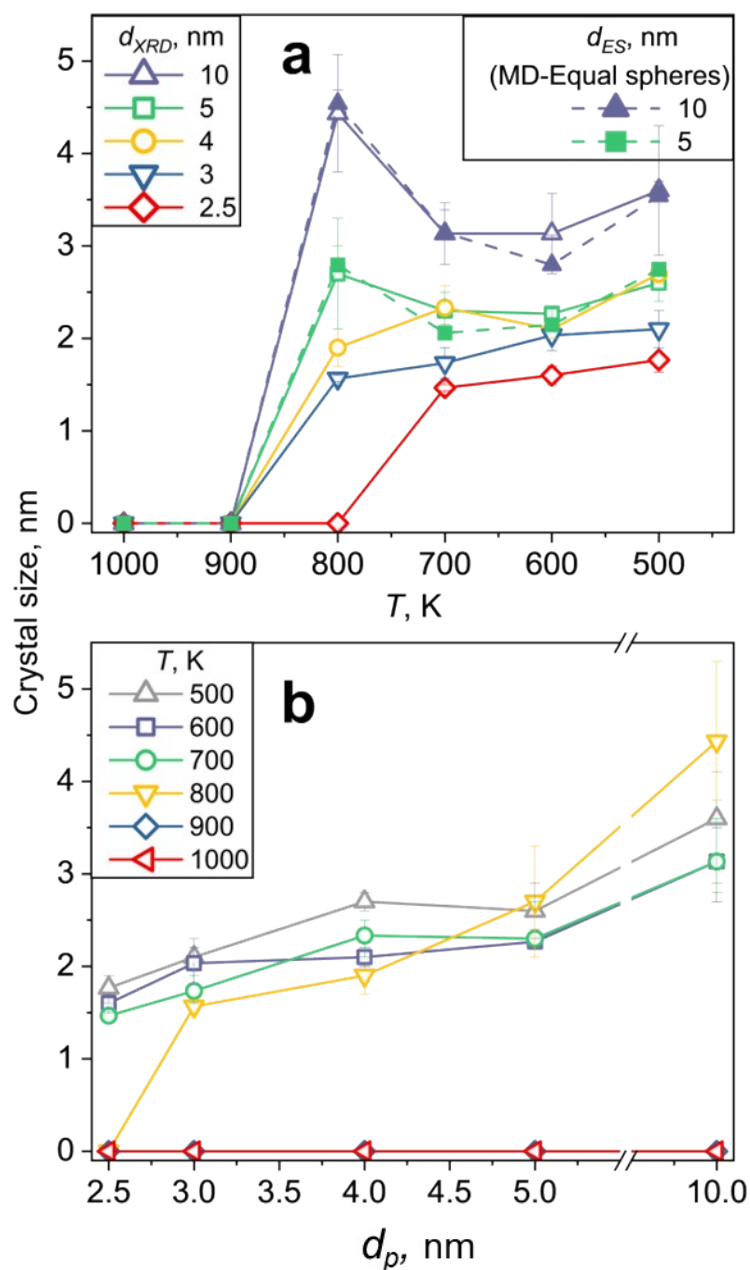


**Figure S15.** Average Au crystal sizes by fitting of XRD patterns ( $d_{XRD}$ ) and by calculating the equivalent spherical diameter of the crystals ( $d_{ES}$ ) of the initially amorphous Au nanoparticles after isothermal crystallization for 100 ns (a) as a function of temperature having  $d_p = 2.5 - 10$  nm and (b) as a function of various  $d_p$  at  $T = 500 - 1000$  K.

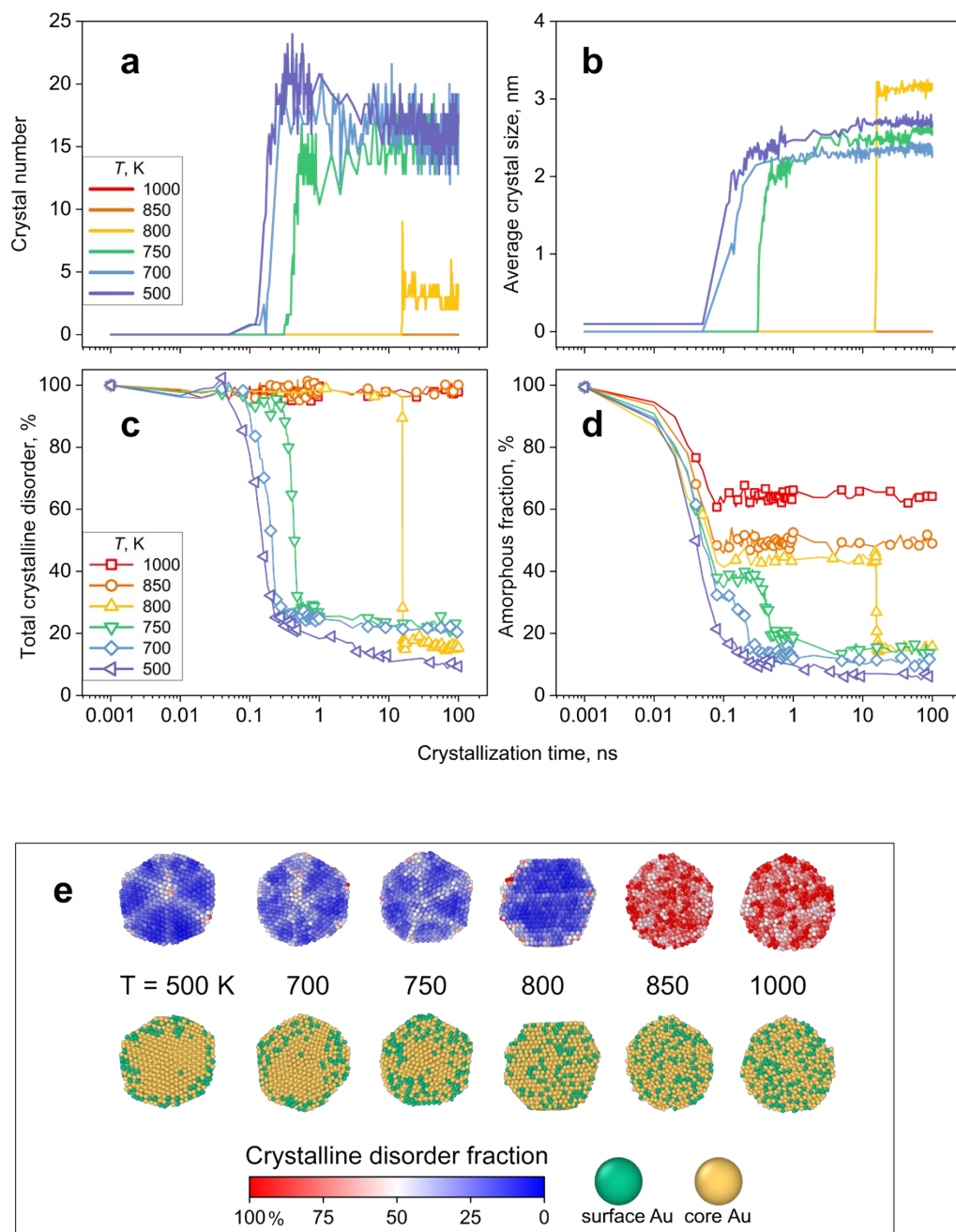


**Figure S16.** Evolution of (a) crystal number, (b) average crystal size, (c) total crystalline disorder fraction, (d) amorphous fraction of initially amorphous Au nanoparticles ( $d_p = 5$  nm) undergoing isothermal crystallization at  $T = 500, 700, 750, 800, 850, 1000$  K and (e) their corresponding snapshots of cross-sections after 100 ns, colored by local crystalline disorder fraction and surface and core Au.



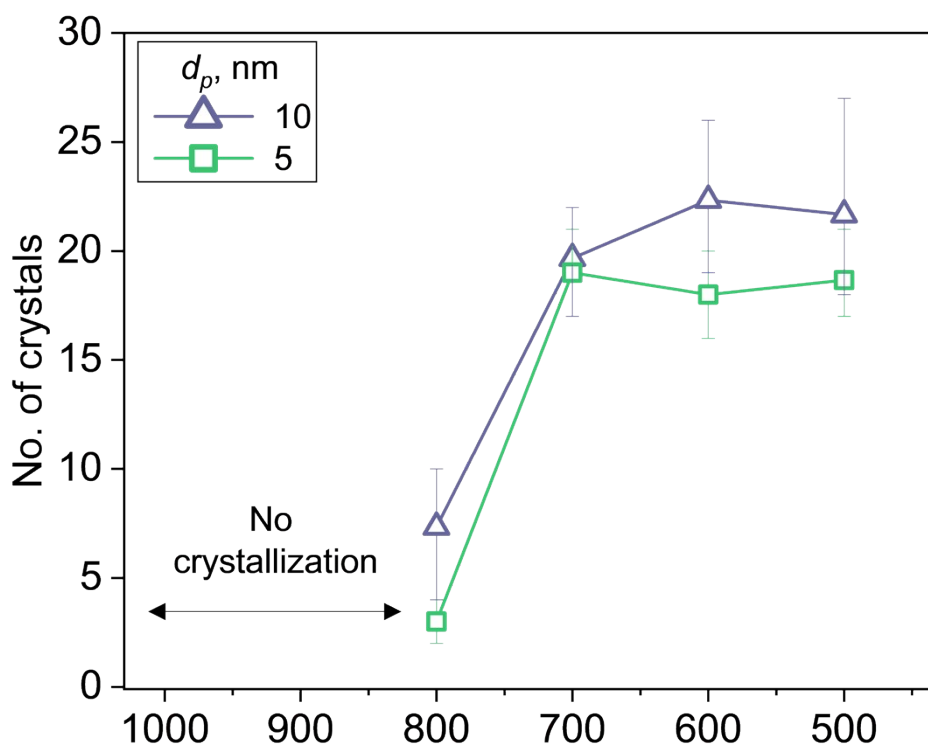


**Figure S17.** number of crystals as a function of temperature for  $d_p = 5$  and 10 nm after crystallization.

Eslami, H.; Sedaghat, P.; Müller-Plathe, F. Local bond order parameters for accurate determination of crystal structures in two and three dimensions. *Phys. Chem. Chem. Phys.* **2018**, 20, 27059-27068. <https://doi.org/10.1039/C8CP05248D>

Quoc, T. T.; Long, V. C.; Talu, S.; Trong, D. N. Molecular Dynamics Study on the Crystallization Process of Cubic Cu-Au Alloy. *Appl. Sci.* **2022**, 12. <https://doi.org/10.3390/app12030946>